Collisions of antiprotons with excited positronium atoms

M. Charlton
Department of Physics, Faculty of Science and Engineering, Swansea University, SA2 8PP, United Kingdom

H. B. Ambalampitiya, I. I. Fabrikant
Department of Physics and Astronomy, University of Nebraska, Lincoln, Nebraska, 68588-0299, USA

D. V. Fursa, A. S. Kadyrov, I. Bray
Curtin Institute for Computation and Department of Physics and Astronomy, Curtin University, GPO Box U1987, Perth, WA 6845, Australia

(Dated: June 21, 2021)

A detailed theoretical investigation of the fundamental three-body antiproton-positronium system is presented, utilising both quantum convergent close coupling and classical trajectory methods. We evaluate scattering cross sections for all major processes, including charge transfer and break-up, over a wide range of positronium kinetic energies and states with principal quantum number $n_{\rm Ps} \leq 6$. The study has significantly extended previous work, and the direct quantum/classical comparison has revealed a systematic approach to obtaining cross sections for arbitrarily high $n_{\rm Ps}$. This is of major significance for prospective applications of collisions of excited positronium atoms in cold (anti-)atomic physics.

PACS numbers: 34.80.-i

The existence of antimatter particles and systems with properties identical in magnitude to those of their ordinary matter counterparts is a fundamental component of the Standard Model of Particle Physics (see, e.g., [1]). The apparent baryon imbalance of the Universe is, however, not encompassed in that framework and constitutes one of the major conundrums of contemporary physics. Detailed matter-antimatter comparisons are, in part, motivated by this as tests of symmetry in nature. Furthermore, experimental studies of the gravitational behaviour of antihydrogen, $\overline{\rm H}$ the positron (e^+)-antiproton ($\overline{p}$) bound state, are under development as antimatter tests of the Equivalence Principle of General Relativity [2–4]. Investigations involving antimatter are typically performed at low energies, using systems carefully prepared under controlled conditions. Nowadays, antiproton and positron capture and manipulation [5] to form, trap and interrogate $\overline{\rm H}$ (see e.g., [6–10]) is routine. Furthermore, several groups have developed the capability to efficiently form clouds of state-selected Rydberg positronium (Ps, the e^+-e^- bound state) atoms in vacuum for further study (see [11] for a review). As a result, progress in $\overline{\rm H}$ and Ps physics has been striking in recent years, which has seen antimatter science cross a threshold: experiment is no longer technique-limited, but driven by applications which impact well beyond a narrow discipline interest. These competencies suggest new avenues of research. Examples include prospects for antimatter chemistry to create more complex objects (for example, $\overline{\rm H}^-$ and $\overline{\rm H}_2^-$ [12, 13], to engender more precise tests of fundamental physics) and the use of charge exchange in collisions involving Ps atoms as a route to novel cold-atom physics and chemistry [14], as well as $\overline{\rm H}$ formation [15]. It is the latter which is of primary interest here, and it is noteworthy that the AEgIS collaboration [16] has recently reported the pulsed production of $\overline{\rm H}$ using the reaction

$$\mathrm{Ps}(n_{\rm Ps}, l_{\rm Ps}) + \overline{p} \rightarrow \overline{\rm H}(n_{\overline{\rm H}}, l_{\overline{\rm H}}) + e^-, \tag{1}$$

where the respective Ps and $\overline{\rm H}$ quantum states are given in the usual notation. A pre-requisite for fully exploiting the promise of Ps collisions is the availability of accurate scattering cross sections, such that guidance from theory is paramount in the assessment of experimental feasibility, and in influencing design to maximize yields from rare reactions. This not only involves data for charge transfer, reaction 1, but also for competing channels such as break-up

$$\mathrm{Ps}(n_{\rm Ps}, l_{\rm Ps}) + \overline{p} \rightarrow \overline{p} + e^+ + e^-, \tag{2}$$

and state-changing collisions

$$\mathrm{Ps}(n_{\rm Ps}, l_{\rm Ps}) + \overline{p} \rightarrow \mathrm{Ps}(n^*_{\rm Ps}, l^*_{\rm Ps}) + \overline{p}, \tag{3}$$

which can alter the useful Ps flux. The Ps-$\overline{p}$ system is a test-bed due to its importance in $\overline{\rm H}$ physics, and since it is possible to perform very accurate quantum calculations that are not feasible for more complex systems. Nevertheless, even the best method available (Convergent Close Coupling, CCC) is restricted in the Ps quantum levels that can be investigated, prompting comparison with scattering methods based upon classical physics, which can be extended to higher states and have well-known scaling behaviours. Since experiment has routine access to states and collisions processes which are currently beyond a full quantum description, it is vi-

tal to know in which circumstances data from a classical approach may be adopted. In this study we report treatment of the Ps-$\bar{p}$ system in a range of states up to $n_{\rm Ps} = 6$, including all major scattering channels. The work is by far the most comprehensive to date and provides a unique comparison of the fully self-consistent quantum theory, CCC, with a Classical Trajectory Monte Carlo (CTMC) approach.

The two-center CCC approach to e^+-H scattering [17, 18] is used to obtain the required integrated cross sections $\sigma_{n_f l_f, n_{\rm Ps} l_{\rm Ps}}$, where $1 \le n_{\rm Ps} \le 6$ and $0 \le l_{\rm Ps} \le n_{\rm Ps} - 1$. The final states correspond to the n_f of atomic and Ps states, which include the representation of the continuum via positive-energy Ps pseudostates allowing the estimation of the break-up cross sections. The atomic states included were those of principal quantum number $n_{\overline{\rm H}} \le 13$ for $l_{\overline{\rm H}} \le 8$. The Ps states were obtained by diagonalization of the Ps Hamiltonian in a Laguerre basis of $N_l = 30 - l$ for $l \le 6$. Full details of the CCC calculations will be given elsewhere, but suffice to say that these are by far the largest two-center CCC calculations undertaken, superseding those of Kadyrov *et al.* [19] not just in the principal quantum numbers considered, but also due to the inclusion of the Ps continuum.

The amount of data generated is very large and some aggregation is necessary for the purpose of presentation of key features. Accordingly, utilizing the degeneracy of the Ps discrete energy levels we eliminate $l_{\rm Ps}$-dependence in the cross sections by averaging over the initial $l_{\rm Ps}$ states and summing over the final l_f via

$$\sigma_{n_f, n_{\rm Ps}} = \sum_{l_f=0}^{n_f-1} \sum_{l_{\rm Ps}=0}^{n_{\rm Ps}-1} \sigma_{n_f l_f, n_{\rm Ps} l_{\rm Ps}} (2l_{\rm Ps}+1)/n_{\rm Ps}^2. \qquad (4)$$

Then the total antihydrogen formation cross section is

$$\sigma^{\overline{\rm H}}_{n_{\rm Ps}} = \sum_{n_{\overline{\rm H}}} \sigma_{n_{\overline{\rm H}}, n_{\rm Ps}}, \qquad (5)$$

where the sum is over all open negative-energy antihydrogen states. The total break-up cross sections is similarly defined, but with the sum being over all open positive-energy Ps states.

In the CTMC approach, first, an initial ensemble of Ps states for a fixed $n_{\rm Ps}$ was generated by random selection on the eccentricity and orientation of the Ps atom (Kepler orbits) [20]. This was repeated for each Ps impact parameter. The classical trajectories from the ensemble were then propagated towards the target. After allowing sufficient interaction times with the target, the final energies and angular momenta of the trajectories were checked to identify the different exit channels. For example, if the final energy left in the relative motion of $\bar{p}$-e^+ pair was negative, then the exit state was counted as an event of antihydrogen formation. Thus, the classical probability for charge transfer as a function of the impact parameter could be obtained by a ratio between the number of trajectories leading to anti-atom formation and the total number of sampled trajectories. The charge-transfer cross section could next be obtained by integrating the probabilities over a range of impact parameters. A similar procedure was implemented to calculate Ps break-up and state-changing cross sections. The current CTMC results were obtained by running about 5000 trajectories for each impact parameter.

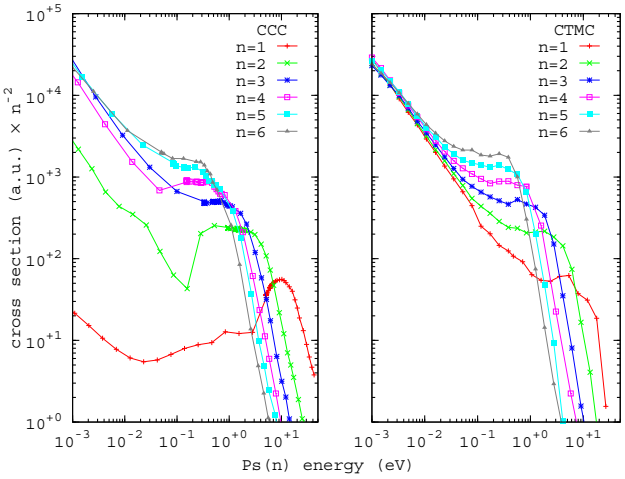

FIG. 1. Total antihydrogen formation cross sections for $\bar{p}$-Ps(n) scattering, scaled by n^{-2} (see text). The CCC data are shown in the left panel, with those for the CTMC approach on the right.

Starting with reaction 1, results for $\overline{\rm H}$ formation for each $n_{\rm Ps}$, as a function of Ps($n_{\rm Ps}$) kinetic energy E, are shown in figure 1 for both CCC and CTMC approaches, scaled by $n_{\rm Ps}^{-2}$ (see below). The energy range $10^{-3} \le E \le 50$ eV was chosen to cover experimental interest. The $n_{\rm Ps} \le 3$ CCC results agree well with the much smaller calculations presented earlier [18]. For $n_{\rm Ps} = 1$ the Ps-$\bar{p}$ interaction is of a short range, therefore the low-energy behavior of the charge-transfer reaction is described by different threshold laws in classical and quantum mechanics: $1/E$ in the former case [21] and the Wigner threshold law $1/E^{1/2}$ [22] in the latter. The situation changes when Ps is initially in an excited state. Then the long-range interaction between Ps and $\bar{p}$ is dominated by the dipolar force [23] due to the degeneracy of excited states with different angular momenta, such that both classical and quantum mechanics lead to the $1/E$ law [24, 25], which allows[1] a cross section estimate for an arbitrarily small E.

According to the classical scaling law [20], the cross

[1] Note that due to the relativistic splitting between the $n_{\rm Ps} l_{\rm Ps}$ levels with different $l_{\rm Ps}$, the energy dependence of the cross section in the ultra-low energy region gradually switches from the $1/E$ to the $1/E^{1/2}$ behavior [26].

section as a function of $n_{\rm Ps}$ and collision energy E generally behaves as

$$\sigma(n_{\rm Ps}, E) = n_{\rm Ps}^4 \sigma(1, n_{\rm Ps}^2 E). \quad (6)$$

For reactions with the $1/E$ energy dependence this results in $n_{\rm Ps}^2$ dependence of the cross section for a fixed energy, which is the scaling employed in Fig. 1.

While there is a quantitative difference between the CCC and CTMC results for $n_{\rm Ps} \leq 2$, it quickly diminishes for higher $n_{\rm Ps}$, in accordance with the generalized correspondence principle of Abrines and Percival [27]. Indeed there is generally good accord for $n_{\rm Ps} \geq 3$. The CCC/CTMC agreement at the low energies of interest to experiment allows the estimation of cross sections for arbitrarily high $n_{\rm Ps}$.

Turning to reactions 2 and 3, the corresponding CCC and CTMC break-up and state-changing cross sections (averaged over the relevant $l_{\rm Ps}$, and scaled by $n_{\rm Ps}^{-4}$) are shown along with the $\overline{\rm H}$ formation data in figure 2. The Ps kinetic energy threshold for break-up is given (in eV) by $6.8/n_{\rm Ps}^2$, whilst that for endothermic state-changing processes (reaction 3, with $n_{\rm Ps}^* > n_{\rm Ps}$) is $6.8(2n_{\rm Ps}+1)/[n_{\rm Ps}(n_{\rm Ps}+1)]^2$. (Note that $\overline{\rm H}$ formation when $\sqrt{2}n_{\rm Ps} > n_{\bar{\rm H}}$ and reaction 3 with $n_{\rm Ps}^* < n_{\rm Ps}$ are exothermic.)

For $n_{\rm Ps} \geq 3$ the endothermic state-changing cross section dominates over those for break-up and for the exothermic process(es) for all kinetic energies other than just above threshold. While for $n_{\rm Ps} = 2$ and 3 the CCC and CTMC data are in general accord for processes other than $\overline{\rm H}$ formation, for $n_{\rm Ps} \geq 4$ the break-up cross sections for CCC fall progressively below those for CTMC: by $n_{\rm Ps} = 6$ the discrepancy is around a factor of 3 at the cross section maximum. This discrepancy has been investigated, and is due to the fact that for the larger initial $n_{\rm Ps}$ convergence in the CCC results requires excitation of positive-energy states with $l_{\rm Ps} \gg 6$. Thus, for estimating break-up cross sections for $n_{\rm Ps} \geq 4$ we recommend the usage of the presented CTMC cross sections, which satisfy the scaling of Eq. (6) reasonably well.

According to the classical scaling law of Eq. (6), the CTMC cross section for Ps break-up peaks at the energy $E_n = E_1/n_{\rm Ps}^2$, where E_1 is the peak energy for $n_{\rm Ps} = 1$, and the peak value grows as $n_{\rm Ps}^4$. This is confirmed by our calculations. A similar scaling is observed for the endothermic case of reaction 3. Overall scaling for the exothermic case is similar to that of reaction 1, although some deviations in CTMC results are observed due to the enforced quantization of the energy spectrum for the final state. Specifically, we assume that the final state belongs to the manifold with the principal quantum number n^* if

$$n^* - 0.5 < n_{\rm eff}^* < n^* + .5$$

where $n_{\rm eff}^* = 1/(2|E_{\rm Ps}|^{1/2})$, and where $E_{\rm Ps}$ is the Ps binding energy in a.u..

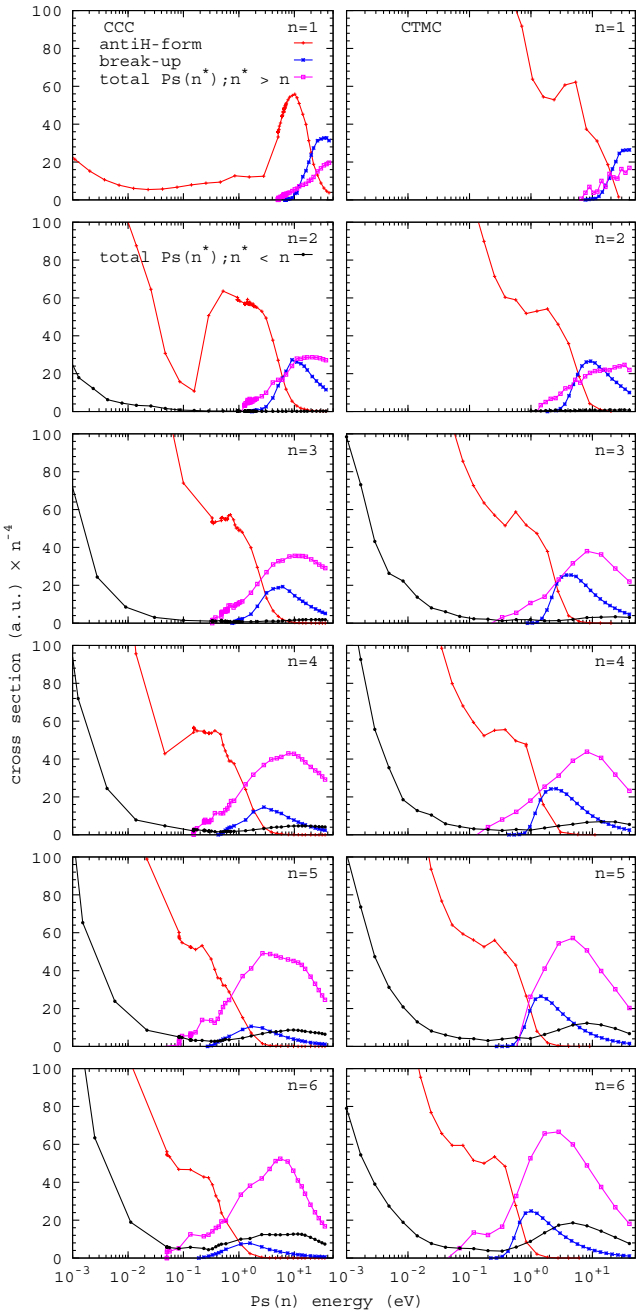

FIG. 2. Integrated cross sections, scaled by n^{-4}, for break-up (reaction 2) and Ps state-changing (reaction 3) for both endo- ($n^* > n$) and exothermic ($n^* < n$) cases (see text) compared to the values for $\overline{\rm H}$ formation of Fig. 1.

There are several immediate consequences of this work for experiment. The GBAR Collaboration plans to use ultra-cold $\overline{\rm H}$ for gravitation studies using the antihydrogen positive ion as an intermediary [3, 28]. The latter is to be produced via a double charge exchange process using a keV energy $\bar{p}$ beam crossing a pulsed Ps target, excited to either the $n_{\rm Ps} = 2$ or 3 levels. The first charge exchange results in $\overline{\rm H}$ formation (reaction 1), with the second proceeding via an $\overline{\rm H}$-Ps reaction, with the antihydrogen in its ground (1S) state (see e.g., [29–31]). The

antihydrogen ion yield depends upon a number of factors, in large part governed by the time-dependencies of the density and the quantum state of the Ps atoms and their interactions to produce $\overline{\mathrm{H}}$, and its subsequent evolution and interaction to form the anti-ion. Our work has shown that the $\overline{p}$-Ps interactions will modify the Ps(n_{Ps}) population and thereby the resulting antihydrogen ion yields, and that such effects will be dependent upon the Ps kinetic energy (or the equivalent for the antiproton) and its initial state. For instance, if n_{Ps} is raised and E lowered in an effort to enhance anti-atom(ion) yields, a more complex set of reaction outcomes need to be considered to provide reliable estimates of yields.

Applications of Ps collisions [14, 16] typically anticipate the use of Rydberg states to enhance the production rate of target species, and as a means of introducing some final state selectivity. The aforementioned threshold behaviour of reaction 1, resulting at fixed E in the n_{Ps}^2 scaling of the cross section, has profound implications on kinetic energy requirements, and may necessitate the development of cryogenic Ps sources and/or the implementation of laser cooling [32, 33].

The underlying physics described herein, and encapsulated by figures 1 and 2, is likely to be similar for any singly positively charged ionic species interacting with positronium. Thus, the current data, being for the equivalent Ps-p^+ system, can be used as a proxy to make estimates for the production rate of cold atoms via charge exchange in Ps-ion collisions [14].

The combined usage of quantum and classical approaches presented here, together with the fundamental threshold and scaling laws, as well as the correspondence principle, allows for the estimate of Ps(n_{Ps})-$\bar{p}$ collision cross sections at all energies of interest to experiment, and for arbitrarily high n_{Ps}. For brevity of presentation, dependence on l_{Ps} has not been considered here, but will be presented elsewhere.

The Curtin authors acknowledge the Texas Advanced Computing Center (TACC) at The University of Texas at Austin and DUG Technology of Perth, Western Australia for providing HPC resources, and also the support of the Australian Research Council, the National Computing Infrastructure and The Pawsey Supercomputer Center. MC thanks the EPSRC (UK) for supporting his antihydrogen research. HA and IIF were supported by the US National Science Foundation under Grant No. PHY-1803744 and by resources of the Holland Computing Center of the University of Nebraska, which receives support from the Nebraska Research Initiative.

[1] M. Charlton, S. Eriksson, and G. M. Shore, "Antihydrogen and fundamental physics," (Springer, 2020) pp. 1–95.

[2] P. Scampoli and J. Storey, Modern Physics Letters A **29**, 1430017 (2014), https://doi.org/10.1142/S0217732314300171.

[3] P. Pérez *et al.* (GBAR Collaboration), Hyperfine Interact. **233**, 21 (2015).

[4] W. A. Bertsche, Philosophical Transactions of the Royal Society A: Mathematical, Physical and Engineering Sciences **376**, 20170265 (2018), https://royalsocietypublishing.org/doi/pdf/10.1098/rsta.2017.0265.

[5] M. Ahmadi, B. X. R. Alves, C. J. Baker, W. Bertsche, A. Capra, C. Carruth, C. L. Cesar, M. Charlton, S. Cohen, R. Collister, S. Eriksson, A. Evans, N. Evetts, J. Fajans, T. Friesen, M. C. Fujiwara, D. R. Gill, J. S. Hangst, W. N. Hardy, M. E. Hayden, C. A. Isaac, M. A. Johnson, S. A. Jones, S. Jonsell, L. Kurchaninov, N. Madsen, M. Mathers, D. Maxwell, J. T. K. McKenna, S. Menary, T. Momose, J. J. Munich, K. Olchanski, A. Olin, P. Pusa, C. O. Rasmussen, F. Robicheaux, R. L. Sacramento, M. Sameed, E. Sarid, D. M. Silveira, C. So, G. Stutter, T. D. Tharp, J. E. Thompson, R. I. Thompson, D. P. van der Werf, and J. S. Wurtele (ALPHA Collaboration), Phys. Rev. Lett. **120**, 025001 (2018).

[6] W. A. Bertsche, E. Butler, M. Charlton, and N. Madsen, J. Phys. B: At. Mol. Opt. Phys. **48**, 232001 (2015).

[7] M. Ahmadi, B. Alves, C. Baker, and et al (ALPHA Collaboration), Nat. Comm. **8**, 681 (2017).

[8] M. Ahmadi, B. Alves, C. Baker, and et al (ALPHA Collaboration), Nature **561**, 211 (2018).

[9] M. Ahmadi, B. Alves, C. Baker, and et al (ALPHA Collaboration), Nature **557**, 71 (2018).

[10] C. Baker, W. Bertsche, A. Capra, and et al. (ALPHA Collaboration), Nature **592**, 35–42 (2021).

[11] D. B. Cassidy, Euro. J. Phys. D **72**, 53 (2018).

[12] E. G. Myers, Phys. Rev. A **98**, 010101 (2018).

[13] M. C. Zammit, M. Charlton, S. Jonsell, J. Colgan, J. S. Savage, D. V. Fursa, A. S. Kadyrov, I. Bray, R. C. Forrey, C. J. Fontes, J. A. Leiding, D. P. Kilcrease, P. Hakel, and E. Timmermans, Phys. Rev. A **100**, 042709 (2019).

[14] W. A. Bertsche, M. Charlton, and S. Eriksson, New J. Phys. **19**, 053020 (2017).

[15] M. Charlton, Phys. Lett. A **143**, 143 (1990).

[16] C. Amsler, M. Antonello, and A. Belov (AEgIS), Phys. Comm. **4**, 19 (2021).

[17] A. S. Kadyrov and I. Bray, Phys. Rev. A **66**, 012710 (2002).

[18] A. S. Kadyrov, C. M. Rawlins, A. T. Stelbovics, I. Bray, and M. Charlton, Phys. Rev. Lett. **114**, 183201 (2015).

[19] A. S. Kadyrov, I. Bray, M. Charlton, and I. I. Fabrikant, Nature Commun. **8**, 1544 (2017).

[20] R. Abrines and I. C. Percival, Proceedings of the Physical Society **88**, 861 (1966).

[21] R. Côté, E. J. Heller, and A. Dalgarno, Phys. Rev. A **53**, 234 (1996).

[22] E. P. Wigner, Phys. Rev. **73**, 1002 (1948).

[23] M. Gailitis and R. Damburg, Proc. Phys. Soc. (London) **82**, 192 (1963).

[24] D. Krasnicky, G. Testera, and N. Zurlo, Journal of Physics B: Atomic, Molecular and Optical Physics **52**, 115202 (2019).

[25] H. B. Ambalampitiya, D. V. Fursa, A. S. Kadyrov, I. Bray, and I. I. Fabrikant, Journal of Physics B: Atomic, Molecular and Optical Physics **53**, 155201 (2020).

[26] I. I. Fabrikant, A. W. Bray, A. S. Kadyrov, and I. Bray, Phys. Rev. A **94**, 012701 (2016).

[27] R. Abrines and I. C. Percival, Proceedings of the Physical Society **88**, 873 (1966).
[28] P. Pérez and Y. Sacquin, Class. Quant. Grav. **29**, 184008 (2012).
[29] P. Comini and P.-A. Hervieux, New J. Phys. **15**, 095022 (2013).
[30] P. Comini, P.-A. Hervieux, and F. Biraben, Hyperfine Interact. **228**, 159 (2014).
[31] T. Yamashita, Y. Kino, E. Hiyama, S. Jonsell, and P. Froelich, New Journal of Physics **23**, 012001 (2021).
[32] K. Shu, X. Fan, T. Yamazaki, T. Namba, S. Asai, K. Yoshioka, and M. Kuwata-Gonokami, Journal of Physics B: Atomic, Molecular and Optical Physics **49**, 104001 (2016).
[33] P. Yzombard, *Laser cooling and manipulation of antimatter in the AEgIS experiment*, Ph.D. thesis, L'Université Paris-Saclay (2016).